Digital Object Identifier 10.1109/ECCE44975.2020.9236136

2020 IEEE Energy Conversion Congress and Exposition (ECCE)

Modular Smart Transformer Topology for the Interconnection of Multiple Isolated AC and DC Grids

Johannes Kuprat

Markus Andresen

Vivek Raveendran

Marco Liserre

Suggested Citation

J. Kuprat, M. Andresen, V. Raveendran and M. Liserre, "Modular Smart Transformer Topology for the Interconnection of Multiple Isolated AC and DC Grids," 2020 IEEE Energy Conversion Congress and Exposition (ECCE), 2020.

Modular Smart Transformer Topology for the Interconnection of Multiple Isolated AC and DC Grids

1st Johannes Kuprat
Chair of Power Electronics
Kiel University
Kiel, Germany
jk@tf.uni-kiel.de

2nd Markus Andresen
Chair of Power Electronics
Kiel University
Kiel, Germany
ma@tf.uni-kiel.de

3rd Vivek Raveendran
Chair of Power Electronics
Kiel University
Kiel, Germany
vir@tf.uni-kiel.de

4th Marco Liserre
Chair of Power Electronics
Kiel University
Kiel, Germany
ml@tf.uni-kiel.de

***Abstract*—The Smart Transformer enables the interconnection of multiple AC and DC grids with potentially different voltage levels. In most configurations, each grid needs to be isolated for preventing the propagation of faults. Actual literature mostly considers a single isolated interconnection, which is not optimized for the interconnection of multiple AC and DC grids. By utilizing the modularity of the Cascaded H-Bridge (CHB) converter and the corresponding connected Dual Active Bridge (DAB) to each H-bridge, this work proposes a system design for feeding multiple AC and DC grids. Requirements for the DC grid isolation and integration are discussed and the proposed topology is demonstrated to enable reduced losses compared to the commonly adopted configuration. The commonly adopted and the proposed configuration are compared and experimental results validate reduced losses for a large range of operation compared to the conventional solution.**

***Index Terms*—Smart Transformer, Hybrid Grid, Low Voltage (LV) DC, Cascaded H-Bridge (CHB)**

I. Introduction

The increasing integration of renewable energy sources and electric vehicle charging stations encourages the use of DC grids, whereby today's transmission and distribution is mostly adopted in AC [1]. A possible solution for the interconnection of an AC and a DC grid has been proposed [2]. However, those connections are not optimum for the interconnection of multiple grids, because multiple power converters are needed for the interconnection of the grids. Alternatively, a centralized solution for the integration of DC grids in the AC infrastructure is the Smart Transformer (ST), which is a solid state transformer with its control and communication capability and it can provide DC-connectivity in Low Voltage (LV) and Medium Voltage (MV) levels [3], [4].

Smart Transformer topologies have been proposed to interconnect MVAC-, LVAC- and LVDC grids. However, no optimization of the interconnection to isolated dc grids has been made so far and even the direct connection of the DC grid to a LVDC link has been proposed [4]–[6]. Apart from the isolation, the controllability is an important requirement in most applications of DC grids, which cannot be provided in this configuration. A simple solution for the connection of the

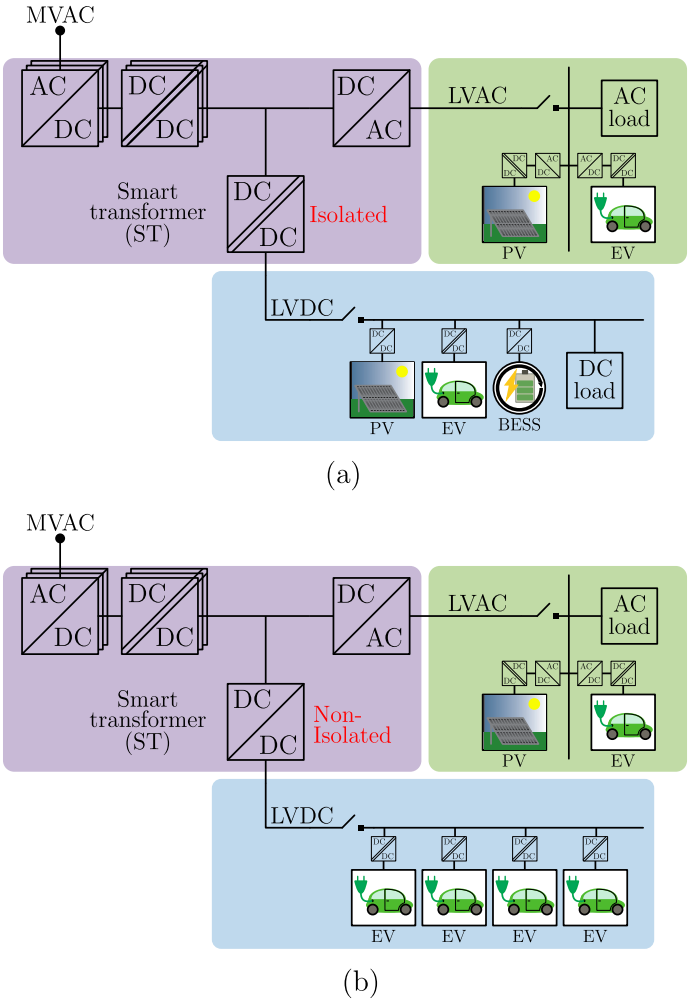

Fig. 1. Scheme of a Smart Transformer with isolation (a) and without isolation (b) between LVAC and LVDC.

DC grid is the use of an isolated DC/DC converter connected to the DC-link, which is shown in Fig. 1 (a). This fulfills the requirements, but power transfer from MVAC to LVDC is conducted through two medium frequency transformers,

which is expected to deteriorate the efficiency of the power conversion.

This work proposes a DC-multibus topology based on a cascaded H-bridge (CHB) converter and dual active bridges, which are connected to a LVDC grid and a DC-link for feeding an AC grid. This solution is compared by means of efficiency to the commonly adopted solution, where the DC grid is fed by an isolated DC/DC converter from the DC-link. The experimental results demonstrate the effectiveness of the proposed solution for a wide range of operating points.

This work first introduces different grid configurations without the need for isolation and with the need for isolation in section II. Section III introduces the proposed topology and compares the efficiency to the commonly adopted solution. Section IV shows preliminary measurements on a test bench before concluding the work in section V.

II. LVDC GRID INTEGRATION REQUIREMENTS

The system design for the integration of LVDC grids through the Smart Transformer is driven by the requirements of the connected grid. In DC distribution grids, the voltage needs to be controllable and isolation is a key requirement. A Smart Transformer topology, which fulfills these demands is shown in Fig. 1 (a). Only in the case that purely isolated loads are connected to the DC grid, such as electric vehicle charging stations, no galvanical isolation is needed as shown in Fig. 1 (b).

As the most important feature of the isolation, disturbances can be prevented from passing through the grids and it prevents high fault and body currents [7]–[9]. In the case with isolation, high resistance grounding schemes can be applied to provide a safer operation of the LVDC grid. While in the non-isolated case, the produced common mode voltage between the LVDC and the LVAC grids will promote high fault and dangerous body currents. So applying galvanic isolation between the LV grids in the ST will improve the safety of personnel and equipment.

Additionally, galvanic isolation between the LVDC and the LVAC grids provides a flexible grounding scheme selection for the LVDC and LVAC grids. Since combinations of low impedance grounding schemes in both LV grids can make the normal operation of the system impossible if no galvanic isolation between them is applied [10]. So the compatibility to several grounding configurations through the galvanic isolation can be a valuable feature of the ST. Especially in the case that the LVDC and the LVAC grids are designed beforehand and just a suitable ST is selected.

As disadvantages of galvanic isolation between the LVDC and the LVAC grids, a higher component count for the converter is required and it potentially reduces the efficiency and increases the volume of the system. These disadvantages additionally relate to the costs of the ST, whereby, the higher purchase costs are initially incurred and possibly reduced efficiency will increase the operating costs. The increased volume will increase costs for the housing of the ST.

TABLE I
RATING OF THE ADVANTAGES AND DISADVANTAGES OF GALVANIC ISOLATION BETWEEN LVDC AND LVAC

Advantages/Disadvantages	Rating
Flexible grounding scheme selection	+
Prevent disturbances passing through grids	++
Prevent high fault and body currents	+++
Higher purchase costs	−
Higher volume	−
Lower efficiency	−−

The rating in Table I shows the high significance of the advantages of the galvanic isolation between LVDC and LVAC. Thus, the safety of persons and equipment should be prioritized compared to the costs. Therefore, an isolating DC/DC converter should be used between the DC grid and the LVDC link of the ST, if also non-isolated loads or non-isolated distributed generators are connected to the DC grid.

III. PROPOSED OPTIMIZED MODULAR ST TOPOLOGY WITH ISOLATED DC GRID

The integration of DC grids in modular STs can be made with an isolated DC/DC converter connected to a DC-link of a three stage Smart Transformer as shown in Fig. 2 (a). The basic structure of the ST is chosen according to [4] as a three-stage configuration with a Cascaded H-Bridge (CHB) for the AC/DC conversion on the MVAC side, followed by Dual Active Bridges (DABs) for the DC/DC conversion, which also provide galvanic isolation between the MVAC and the LV grids, and an inverter for the provision of LVAC grid. For applying galvanic isolation between the LVAC and the LVDC grid, a DAB, which is providing the LVDC grid, is connected to the DC-link. In the following, this is referred as Non-Interconnected Topology (NIT) as illustrated in Fig. 2 (a).

This topology provides galvanic isolation between all connected grids, but for power transfer from the MVAC grid to the LVDC grid, the power is transferred through two transformers, which raises concerns against excessive losses. For this reason, the Interconnected Topology (IT), as illustrated in Fig. 2 (b) is proposed. In the IT, a certain number of the DABs from the CHB are connected directly to the LVDC feeder and the DAB between the LV DC-link and the LVDC feeder is building an interconnection. In the IT, it is possible to transfer power from the MVAC to the LVDC grid with only two conversion stages, including only one transformer, instead of the three, including two transformers, in the NIT. Therefore, it is expected to achieve higher efficiency in many operating points besides the improved fault tolerance for the LVDC grid.

In order to quantify the performance of the proposed topology compared to the commonly adopted topology, an efficiency evaluation at all the operating points is required. The procedure used for the evaluation of the efficiency is illustrated in Fig. 3. Firstly, the ideal waveforms of the converters dependent on the output power are derived [11]. Secondly,

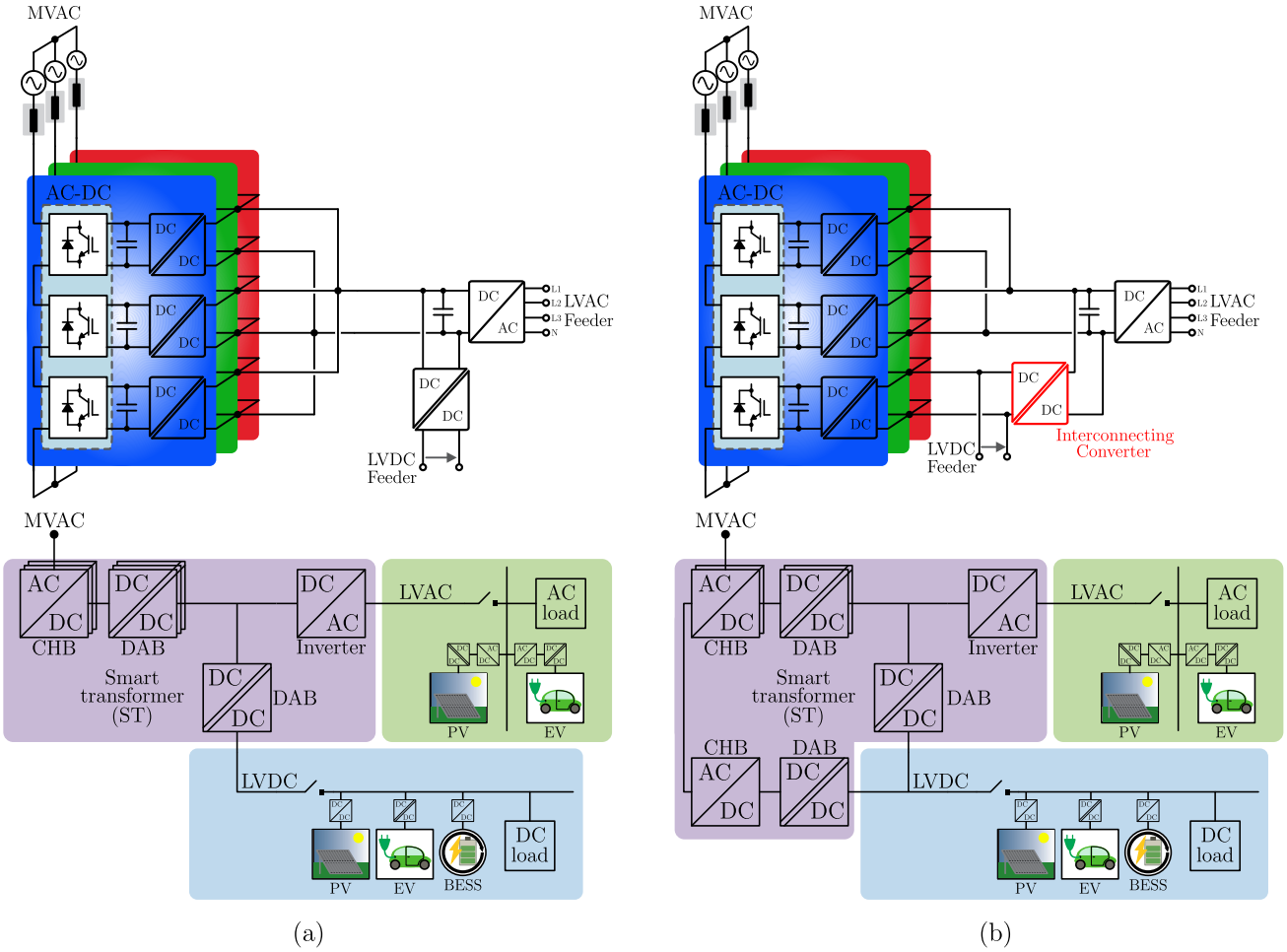

Fig. 2. Structure of the NIT (a) and the IT (b).

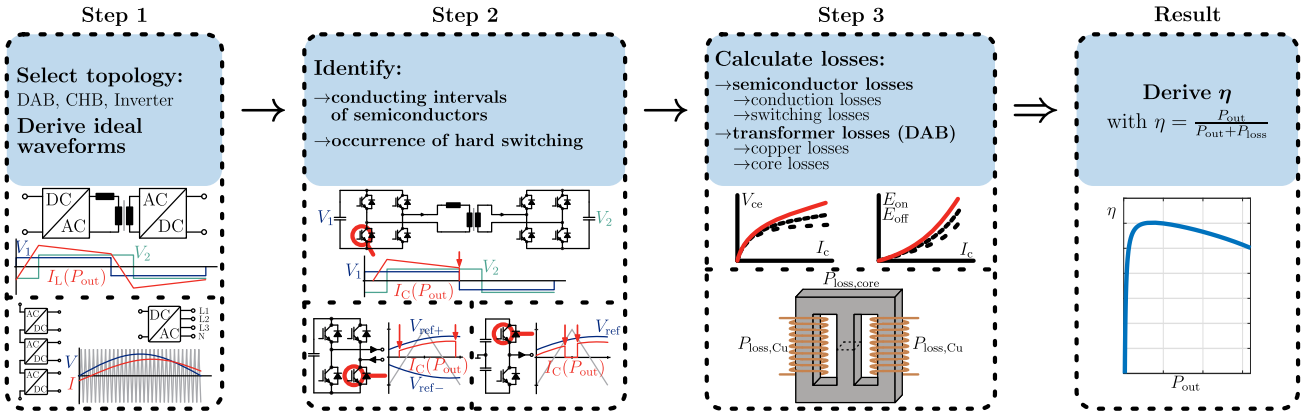

Fig. 3. Modeling procedure to derive efficiency curves of the converters.

the conduction intervals and the occurrence of the switching losses are identified. Thirdly, the semiconductor losses [12] and the transformer losses [11] are calculated. The considered semiconductor modules are listed in Appendix A. So the efficiency curves of the converters can be calculated and used in an analysis of the power flow to calculate the efficiency of the system. The efficiencies of the NIT and the IT depending on the active power of the LVAC grid P_{LVAC} and that of the LVDC grid P_{LVDC} are shown in Fig. 4. The borders of the operating area are done through the power limitations of the different converters, as shown in Fig. 5. It can be recognized that the NIT has a wider operating area when one LV grid is

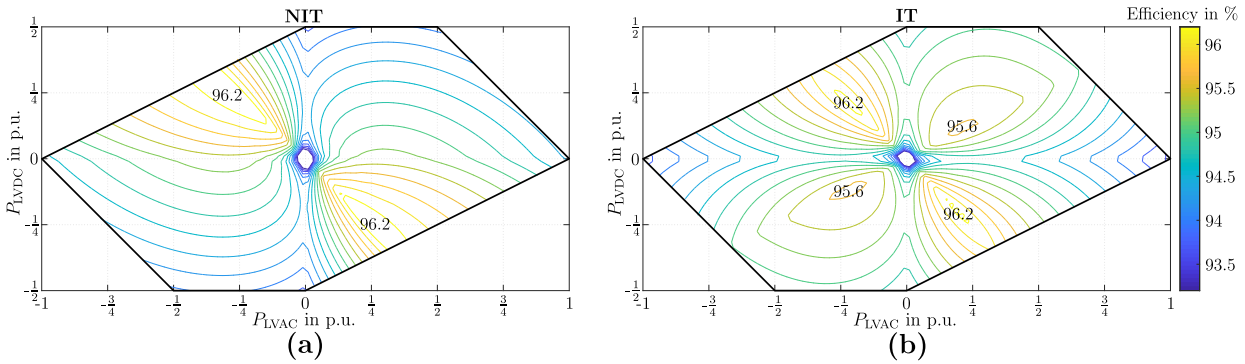

Fig. 4. Efficiency of the NIT (a) and the IT (b) for varying P_{LVAC} and P_{LVDC}.

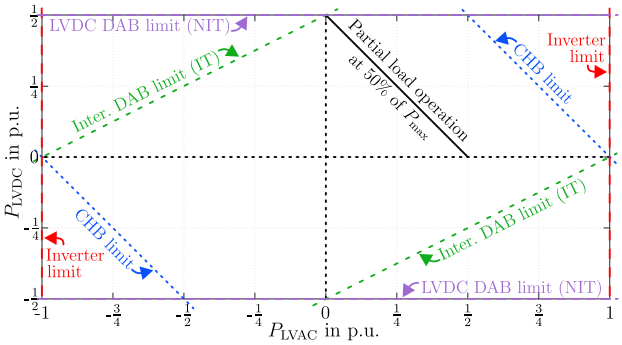

Fig. 5. Borders of the operating area due to the limitations of the different converters and partial load operation at 50 % of P_{max}.

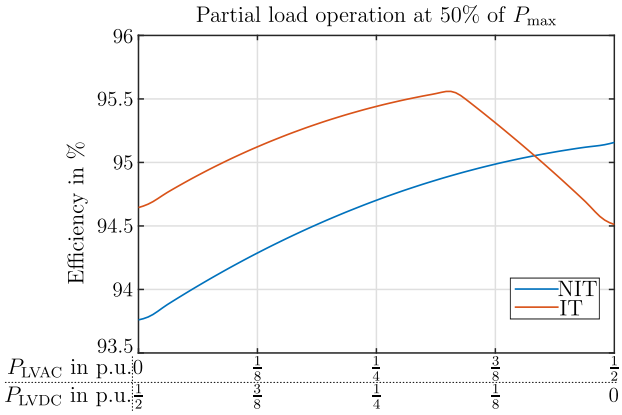

Fig. 6. Efficiencies in the IT and the NIT for partial load operation with varying $\frac{P_{\mathrm{LVAC}}}{P_{\mathrm{LVDC}}}$.

generating power and the other is consuming power. However, to realize the shown operating limitations by the converters the LVDC DAB in the NIT needs to be sized 50 % higher than the interconnecting DAB in the IT. The angle of the border of the operating area due to the interconnecting DAB as well as the sizing of the interconnecting DAB are dependent on how many DABs from the CHB are connected directly to the LVDC feeder.

To compare the efficiencies of the topologies, they are

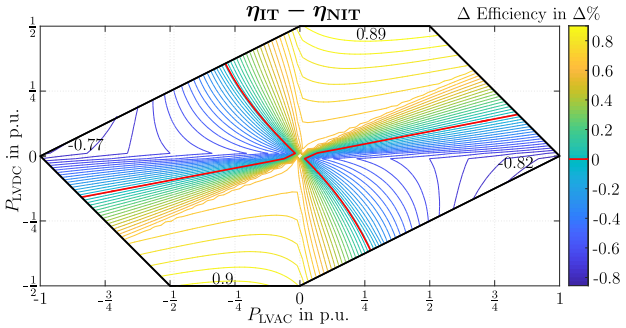

Fig. 7. Comparison of the efficiencies in the IT and the NIT dependent on the operating point.

shown in Fig. 6 in partial load operation at 50 % of the maximum power P_{max} with varying the ratio $\frac{P_{\mathrm{LVAC}}}{P_{\mathrm{LVDC}}}$ while their sum remains the same. The localization of this line in the operating area is shown in Fig. 5. For the identification of the operating area in which the IT provides higher efficiency, the difference between the efficiency of the IT and that of the NIT is shown in Fig. 7. When both LV grids consume power ($P_{\mathrm{LVAC}} > 0 \cap P_{\mathrm{LVDC}} > 0$), the IT is providing higher efficiency for most operating points, up to an efficiency increase of 0.89 %, which corresponds to a reduction of the losses by 15 %. The efficiency peak for the IT in this area can be relocated by adjusting the number of DABs from the CHB connected directly to the LVDC feeder.

Therefore, the IT can bring advantages in terms of efficiency and converter sizing for many use profiles. Further, the results for the considered system are scalable as long as the ratio between the MVAC voltage and the total power of the system is kept constant. Otherwise a different design of the converters needs to be considered, with other semiconductors and transformer design. However, also other designs for the system provide similar results.

IV. Experimental Results

To validate the analytical efficiency comparison between the IT and the NIT, small scale prototypes of both the topologies are tested in the laboratory. Since the CHB converter part is common for both topologies and the major difference lies in

the DAB converter connections, only the part consisting of the DABs connected to the CHB cells and the DAB between the LV DC-link and the LVDC feeder have been considered for loss comparison. The setup of three DABs is shown in Fig. 8 and their configuration for the representation of the part of the NIT and the IT is illustrated in Fig. 10. The equipment used for the validation is shown in Fig. 9.

The parameters in the setup are chosen as shown in Table II. The waveforms of V_{DClink}, V_{LVDC}, the output currents of the DABs, and the voltages on the primary and secondary side of the transformer of the first DAB for the IT configuration are shown in Fig. 11. The losses of the setup are measured with a Yokogawa WT3000E power analyzer. The measurements are carried out so that they can be compared with the partial load operation in Fig. 6. Therefore, the ratio $\frac{P_{\mathrm{LVAC}}}{P_{\mathrm{LVDC}}}$ is varied while their sum stays the same. The measured losses in Fig. 12 confirm that the IT is providing lower losses in the most operating points for partial load operation. This complies with the results from the theoretical analysis. Further, the operating point with the lowest losses respectively the highest efficiency for the IT is localized where the ratio $\frac{P_{\mathrm{LVAC}}}{P_{\mathrm{LVDC}}}$ is equal to the ratio of the number of DABs from the CHB connected to the LVDC link to the number of those connected directly to the LVDC feeder. This is valid for the measurements in the laboratory, for which both these ratios are 1, as well as for the theoretical efficiency analysis, for which these ratios are 2.

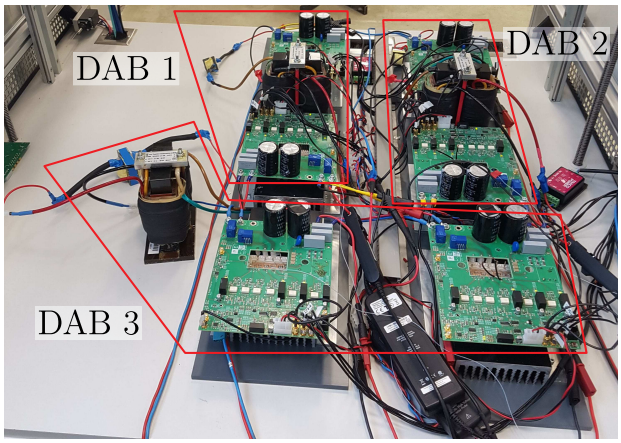

Fig. 8. Setup used for the laboratory validation.

Fig. 9. Equipment used for the laboratory validation.

TABLE II
PARAMETERS OF THE EXPERIMENTAL SETUP

Parameter	Value
V_{s1}, V_{s2}	250 V
V_{DClink}	250 V
V_{LVDC}	250 V
C_{DClink}	1.8 mF
C_{LVDC}	1.8 mF
L_{DAB}	70 µH
$f_{\mathrm{sw,DAB}}$	12 kHz
n_{DAB}	1

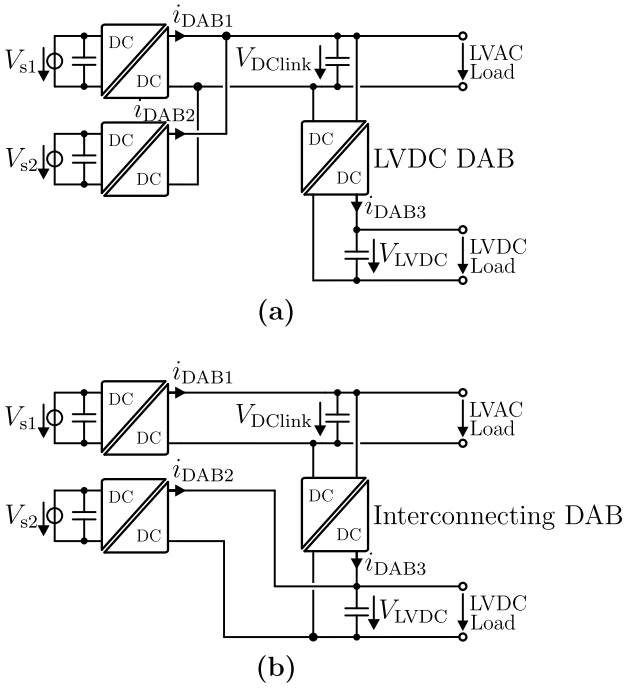

Fig. 10. Scheme of the setup for configuration as NIT (a) and as IT (b).

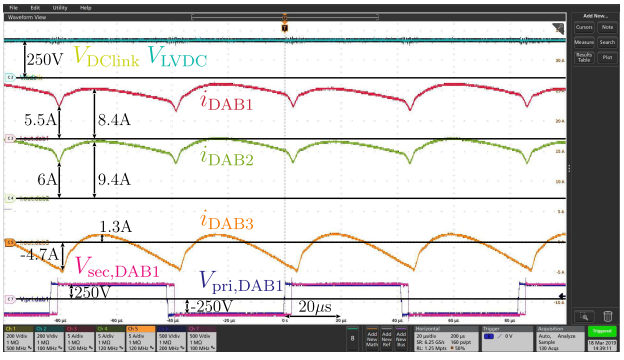

Fig. 11. Waveforms of the laboratory setup configured as the IT.

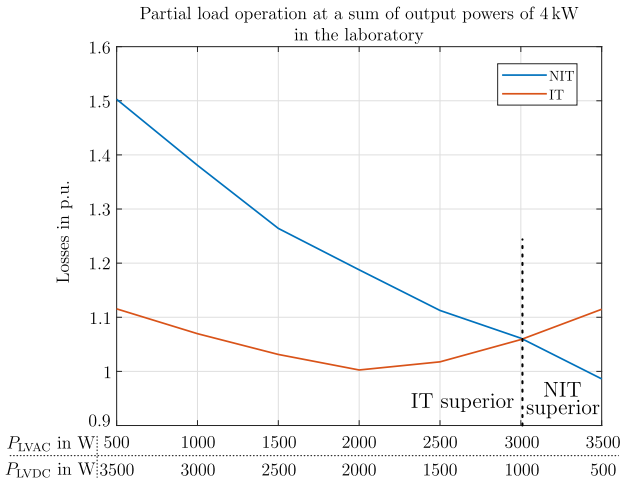

Fig. 12. Losses of the NIT and IT measured in the laboratory (1 p.u. = 650 W).

V. Conclusion

With the increasing emphasis for DC grid integration in the power system, the paper investigates a novel Smart Transformer topology with potentially higher efficiency, better fault tolerance for the LVDC grid and the possibility to downsize a converter compared to the commonly adopted topology. The proposed isolated ST topology takes advantage of the CHB-DAB connections to enable lower number of power conversion stages between MVAC, LVDC and LVAC grids to achieve higher efficiencies at for a wide operation range. The analytical results indicate a loss reduction of up to 15 % with the proposed topology compared to the commonly adopted one. For the assumed scenario, the converter between the LVDC link and the LVDC feeder in the proposed topology can be downsized by 33 % compared to the commonly adopted one. The experimental results validate the potential of a higher efficiency from the analytical findings.

References

[1] A. Gupta, S. Doolla, and K. Chatterjee, "Hybrid ac-dc microgrid: Systematic evaluation of control strategies," *IEEE Transactions on Smart Grid*, vol. 9, no. 4, pp. 3830–3843, July 2018.

[2] H. A. B. Siddique and R. W. De Doncker, "Evaluation of dc collector-grid configurations for large photovoltaic parks," *IEEE Transactions on Power Delivery*, vol. 33, no. 1, pp. 311–320, Feb 2018.

[3] M. Liserre, G. Buticchi, M. Andresen, G. D. Carne, L. F. Costa, and Z. Zou, "The smart transformer: Impact on the electric grid and technology challenges," *IEEE Industrial Electronics Magazine*, vol. 10, no. 2, pp. 46–58, June 2016.

[4] L. F. Costa, G. D. Carne, G. Buticchi, and M. Liserre, "The smart transformer: A solid-state transformer tailored to provide ancillary services to the distribution grid," *IEEE Power Electronics Magazine*, vol. 4, no. 2, pp. 56–67, June 2017.

[5] C. Kumar, Z. Zou, and M. Liserre, "Smart transformer-based hybrid grid loads support in partial disconnection of mv/hv power system," in *2016 IEEE Energy Conversion Congress and Exposition (ECCE)*, Sep. 2016, pp. 1–8.

[6] D. Das, V. Hrishikesan, and C. Kumar, "Smart transformer-based hybrid lvac and lvdc interconnected microgrid," in *2018 IEEE 4th Southern Power Electronics Conference (SPEC)*, Dec 2018, pp. 1–7.

[7] P. Nuutinen, T. Kaipia, J. Karppanen, A. Mattsson, A. Lana, A. Pinomaa, P. Peltoniemi, J. Partanen, M. Luukkanen, and T. Hakala, "Lvdc rules - technical specifications for public lvdc distribution network," *CIRED - Open Access Proceedings Journal*, vol. 2017, no. 1, pp. 293–296, 2017.

[8] T. R. de Oliveira, A. S. Bolzon, and P. F. Donoso-Garcia, "Grounding and safety considerations for residential dc microgrids," in *IECON 2014 - 40th Annual Conference of the IEEE Industrial Electronics Society*, Oct 2014, pp. 5526–5532.

[9] M. Mobarrez, D. Fregosi, S. Bhattacharya, and M. A. Bahmani, "Grounding architectures for enabling ground fault ride-through capability in dc microgrids," in *2017 IEEE Second International Conference on DC Microgrids (ICDCM)*, June 2017, pp. 81–87.

[10] D. Kumar, F. Zare, and A. Ghosh, "Dc microgrid technology: System architectures, ac grid interfaces, grounding schemes, power quality, communication networks, applications, and standardizations aspects," *IEEE Access*, vol. 5, pp. 12 230–12 256, 2017.

[11] V. M. Iyer, S. Gulur, and S. Bhattacharya, "Optimal design methodology for dual active bridge converter under wide voltage variation," in *2017 IEEE Transportation Electrification Conference and Expo (ITEC)*, June 2017, pp. 413–420.

[12] U. Drofenik and J. W. Kolar, "A general scheme for calculating switching- and conduction-losses of power semiconductors in numerical circuit simulations of power electronic systems," *International Power Electronics Conf.*, 2005.

Appendix A

The semiconductor modules of which the characteristic curves were considered in the efficiency analysis are listed in Table III.

TABLE III
IGBT modules from Infineon used for the converter modeling in the efficiency analysis

Converter	IGBT module
Interconnecting DAB	FF50R12RT4
LVDC DAB	FF75R12RT4
DABs in series with the CHB	FP25R12KE3
Inverter	FF200R12MT4
CHB	FP40R12KE3